Reinsch, T., Thurley, T., Jousset, P. (2017): On the mechanical coupling of a fiber optic cable used for distributed acoustic/vibration sensing applications — a theoretical consideration. - *Measurement Science and Technology*, *28*, 12.

DOI: http://doi.org/10.1088/1361-6501/aa8ba4

On the mechanical coupling of a fiber optic cable used for distributed acoustic/vibration sensing applications - a theoretical consideration

Thomas Reinsch, Tom Thurley, Philippe Jousset

GFZ German Research Centre for Geosciences, Telegrafenberg, Potsdam, Germany

E-mail: `Thomas.Reinsch@gfz-potsdam.de`

Abstract. In recent years, fiber optic cables are increasingly used for the acquisition of dynamic strain changes for seismic surveys. When considering seismic amplitudes, one of the first questions arising is the mechanical coupling between optical fiber and the surrounding medium. Here we analyse the interaction of ground movement with a typical telecom-grade fiber optic cable from an existing telecommunication network deployed in a sand filled trench at the surface. Within the cable, the optical fiber is embedded in a gel filled plastic tube. We apply Hooke's law to calculate the stress needed to strain the optical fiber throughout the cable structure. In case the stress magnitude at the cable-sand interface as well as the gel-optical fiber interface is below the yield strength of the respective material, sand and gel, it can be regarded as an elastic medium. Hence, a multilayer radial symmetric model can be used to calculate the coupling of the optical fiber with the surrounding medium. We show that the transfer function has a -3 dB lower cut-off wavelength of about 22 m. The magnitude response of this telecom-grade fiber optic cable is therefore almost perfect at typical low frequency seismic waves. The approach presented here can be applied to various cable designs to estimate the strain transfer between ground movement and an optical fiber.

PACS numbers: 07.60.Vg,93.85.Rt,91.30.Hc,91.30.Dk

Submitted to: *Meas. Sci. Technol.*

Keywords: distributed acoustic/vibration sensing, coupling, seismic survey, seismology, instrumental response

1. Introduction

Fiber optic cables are increasingly used for the acquisition of dynamic strain changes in geophysical applications (e.g. Mestayer et al., 2011; Daley et al., 2013; Götz et al., 2017). This technology is often referred to as distributed acoustic sensing (DAS) or distributed vibration sensing (DVS) (Hartog et al., 2013), where phase-OTDR (optical time domain reflectometry, φ-OTDR) data is used to measure local strain changes at several positions along an optical fiber (Masoudi and Newson, 2016). A coherent laser pulse is coupled into the optical fiber and the phase difference of elastically backscattered photons from neighbouring positions along the fiber can be analysed. When analysing local strain changes, the mechanical coupling of the sensing fiber with the surrounding environment has to be known.

Several studies analysing the strain transfer across to an optical fiber exist (e.g. Pak, 1992; Ansari and Libo, 1998; Schmidt-Hattenberger et al., 2003; Li et al., 2006, 2009). Here, we apply and extend the approach of Li et al. (2006) to analyse the mechanical coupling of an optical fiber inside a standard telecommunication cable deployed in the subsurface. Inside the cable structure, the optical fiber is embedded in a gel, and the gel is confined in a plastic tube. To increase the strength of the fiber optic cable, steel wires are used as strength members. In addition, a plastic outer layer protects the cable from e.g. alteration and corrosion (Refi, 1998). In our application, the fiber optic telecommunication cable is embedded in a trench and covered with sand (Figure 1).

The study is motivated by the continuous acquisition of DAS data along a 15.3 km fiber optic cable within the telecommunication network of Iceland (Reinsch et al., 2016; Jousset et al., 2016) where the mechanical coupling between the optical fiber and the subsurface is unknown, and the cable was not accessible for calibration measurements. Data was collected in the framework of the EC funded FP7 project IMAGE (Integrated Methods for Advanced Geophysical Monitoring) van Wees et al. (2015). To interpret the data, we estimated the strain transfer from the surrounding rock mass to the optical fiber. Information about the multi-layer cable design and its deployment in the 1990's is available, the mechanical properties of individual layers like the gel or the unconsolidated sand surrounding the optical cable, however, are unknown and assumptions have to be made. Evaluating the mechanical properties of sand and gel, we were able to populate the model of Li et al. (2006) and calculate the strain transfer to the optical fiber for seismic applications.

2. Theory

In order to estimate the mechanical coupling between fiber optic cable and the surrounding medium, the force applied to the cable needed to create the measured strain has to be calculated. Assuming elastic rheology, Hooke's Law (Hooke, 1678) is applied:

$$\sigma = \epsilon E \tag{1}$$

where σ is the stress, ϵ the strain and E the Young's modulus. The stress σ is defined as:

$$\sigma = \frac{F}{A} = \epsilon E = \epsilon \frac{k}{A} \tag{2}$$

where F is the force applied to a cross-sectional area A and $k = AE$ is defined as the axial stiffness. For a multilayer cable, the axial stiffness per unit length can be written as:

$$k = \sum_{i=1}^{n} k_i \tag{3}$$

where k_i is the is the axial stiffness for each component i.

2.1. Mechanical coupling with surrounding medium

Here, we consider a fiber optic communication cable, buried in a trench and embedded in sand at a depth of about 1 m. To evaluate whether the sand is plastically or elastically deformed from seismic waves passing the trench, the force necessary to overcome the yield strength of sand at the sand-cable interface is estimated. We assume that (a) the sand can be treated as a homogeneous medium, (b) the contact force between cable and sand is created due to the lithostatic stress, i.e. the weight of the overburden sand, (c) cohesion between individual sand grains is neglected. According to Mohr (1900), the shear strength τ is defined by the Mohr-Coulomb failure criterion:

$$\tau = c + \sigma_N \tan(\varphi) \tag{4}$$

where σ_N is the lithostatic stress normal to the medium, c is a measure of the internal forces and φ is the friction angle. Typical friction angles for non-cohesive sand are are in the order of 30-40° (Grabe, 2012). The lithostatic stress was calculated according to the density ρ of the overburden material and the depth of burial h:

$$\sigma_N = \rho g h \tag{5}$$

For non-cohesive sand ($c = 0$), typical densities are in the range of 1600-2000 kg/m^3 (Grabe, 2012). Consequently, in 1 m depth, the shear strength of the sand can be calculated to be in the range of 9000-16500 Pa. For the interface friction angle of a flat sample of 8in HDPE pipe versus Fraser River sand, Huber (2014) measured about 26° in a direct shear test. The shear strength of the interface between cable and sand is therefore above 7500 Pa.

2.2. Viscosity

Optical fibers inside a fibre optic cable are often embedded in non-Newtonian, oil-based visco-elastic fluid inside a tube. To maintain optical transmission properties over a long time, such fluids are designed to isolate the optical fibers from external forces and to avoid any water migration along the cable. On the one hand, such a gel shall be low viscous to maintain fiber mobility within the cable as well as to allow for an easy

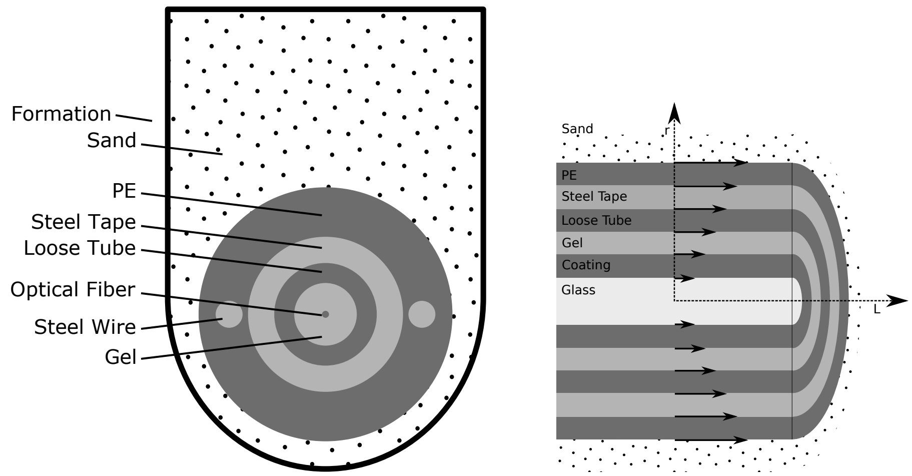

(a) Set-up (b) Cable design

Figure 1. (a) Schematic view of a multilayer fiber optic cable embedded in a sand filled trench. (b) Schematic cross sectional view of the fiber optic cable. Arrows indicates the strain transfer across the cable to the optical fiber. L denotes the length of the cable under investigation and r is the radial distance from the center; dimensions not to scale.

intrusion of the fluid into the tube during cable manufacturing. On the other hand, a high viscosity is desired to avoid the fluid from dripping out of the tube once intruded into it. As a gel with low viscosity is mechanically unstable in a cable structure, a high viscosity gel reduces the ability of the fiber to quickly move relative to the plastic tube in response to external forces. A thixotropic fluid is generally used to protect the optical fibers during movement of the cable (e.g. Khan et al., 1991). For seismic applications, the time of excitation is very short, the thixotropic behaviour will therefore be neglected in the following.

Neglecting creep (e.g. plastic deformation of the gel below the yield strength), different rheological models can be applied to describe such non-Newtonian fluids. One of the most simple models to describe a non-Newtonian fluid is the Bingham fluid model (Bingham, 1916), where a yield strength τ_0 of the gel has to be overcome before it behaves like a viscous fluid:

$$\tau = \tau_0 + \dot{\gamma}\nu_p \tag{6}$$

where τ is the resulting stress to generate a shear rate $\dot{\gamma}$ for a gel with a plastic viscosity ν_p. Another model, taking into account the non linear plastic viscosity of the gel, is the Hershel-Bulkley model (Herschel and Bulkley, 1926):

$$\tau = \tau_0 + K\dot{\gamma}^n \tag{7}$$

where K the consistency factor and n the flow behaviour index. Again, the yield strength τ_0 has to be overcome before the gel behaves like a fluid. Below the yield strength, the fluid behaves like an elastic medium. Typically, gels are engineered to have a yield point of 35-140 Pa (Evonik Industries, 2015). A linear relation between yield point and the elastic modulus of typical gels can be observed. For yield points greater than 30 Pa, an elastic modulus of more than 100 Pa can be assumed (Evonik Industries, 2015).

2.3. Strain Transfer

The strain transfer between the surface of the cable and the optical fiber can be evaluated according to the analytical model of Li et al. (2006). Li et al. (2006) take into account an optical fiber embedded in a perfectly bonded multilayer, radial symmetric design of elastic materials, where stress is uniformly applied to the outside of the system. In this model the boundary condition for the strain measured along the optical fiber is zero at both ends of the investigated cable section. The average strain transfer rate $\overline{\alpha}$ can be estimated according to:

$$\overline{\alpha} = 1 - \frac{\sinh(\beta \frac{L}{2})}{\beta \frac{L}{2} \cosh(\beta \frac{L}{2})} \tag{8}$$

where L is the length of the multilayer system under stress and β is the shear lag parameter:

$$\beta^2 = \frac{2}{r_g^2 E_g \left\{ \sum_{i=1}^{n} \frac{1}{G_i} \ln(\frac{r_i}{r_{i-1}}) \right\}} \tag{9}$$

where r_g and E_g are the outer radius and Young's modulus of the cladding, respectively. For simplicity, it is assumed that core and clad have the same mechanical properties. r_i and G_i is the outer radius and shear modulus of the i-th layer and i=1 denotes the cladding material.

2.4. Experimental set-up in Iceland

In our study the cable has a centrally situated loose tube with a reasonable excess length that minimizes the influence of lateral crush. A double wire acts as strength member to provide sufficient strain resistance. In Iceland, an about 1 m deep trench was dug in solidified basaltic lava. The fiber optic cable was embedded in sand and the trench was re-filled with sand and the excavated lava. Figure 1 shows the model set-up used in this study.

To calculate the mechanical properties of the fiber optic cable, cable dimensions are estimated based on commercially available GYXTW cable types (Table 1). For simplicity, the properties of the steel tape are assumed to be similar to the properties of steel.

For seismic applications, relevant frequencies are typically ranging form 0.1-100 Hz (Aki and Richards, 2002). When a seismic wave passes by, the cable is compressed and stretched with an amount depending on the angle of incidence for the seismic wave as well as the type wave. During our measurement campaign in Iceland, strain magnitudes typically much lower than 1 μm/m were observed.

For every site, the mechanical coupling between the subsurface and the optical fiber has to be evaluated. The workflow to evaluate the strain transfer between surrounding

Table 1. Design of a GYXTW cable together typical young's moduli (E) are given. Cited references are: [1]Ansari and Libo (1998),[2]Evonik Industries (2015),[3]Kern GmbH (2016a),[4]Kern GmbH (2016a), [5]Kuchling (2011),[6]Kern GmbH (2016b). The shear modulus of PE, PBT and the gel was calculated according to $E = 2G(1 + \nu)$ with a Poisson's ratio of $\nu = 0.5$.

Component	Material	Outer Radius (mm)	E (kN/mm^2)	G (kN/mm^2)
Fiber Core	Glas	0.004	72 [1]	
Fiber Clad	Glas	0.0625	72 [1]	
Fiber Coating	Silicon	0.250	2.55e^{-3} [1]	8.50e^{-3} [1]
Tube Filling Compound	Gel	0.9	1e^{-7} [2]	3.3e^{-8}
Loose Tube	PBT	1.3	2.5 [3]	0.83
Steel Tape	Steel	1.43	211 [5]	80 [5]
Outer Sheath	PE	4.25	1.35 [6]	0.45
2 Wires	Steel	0.8	211 [5]	80 [5]

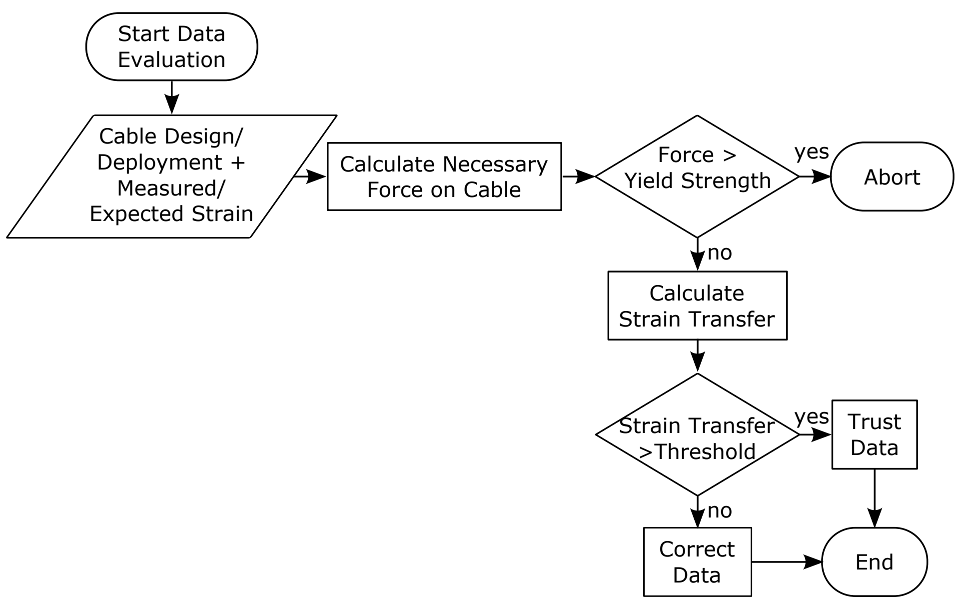

Figure 2. Flow chart showing the procedure to evaluate the mechanical coupling between the subsurface and the optical fiber.

medium and optical fiber is detailed in Figure 2. The single steps are based on equations 1 - 9. The threshold in Figure 2 refers to ground motions, where the mechanical coupling influences measured amplitudes significantly. In our study, we set the threshold to -3 dB. Below the threshold, data must be corrected to compensate the influence of poor coupling.

3. Results

According to the specifications of the fiber optic cable listed in Table 1, the force needed to stretch the cable to 1 μm/m is about 1.2 N (Equations 2 and 3). This force is applied at the surface of the fiber optic cable. The corresponding cable length is more than 10 m for seismic frequencies we observed in Iceland (0.1-50 Hz) and subsurface velocities larger than 700 m/s Raab et al. (2017).

3.1. Mechanical coupling of cable to ground

For a length of more than 10 m, the surface area of the cable is at least 0.28 m^2 (see Table 1). The shear stress at the interface is therefore greater than 4.5 Pa. This value is three orders of magnitude lower than the shear stress needed to shear non-cohesive sand (see Section 2.1).

3.2. Mechanical coupling of optical fiber to cable

Equation 3 can be used to calculate the force acting at the surface of the optical fiber, i.e., at the interface between optical fiber and tube filling compound, here a gel, as well as at the interface between gel and loose tube. With regards to the surface area at each interface, the acting shear stresses are calculated according to Equation 2 to be 0.12 Pa and 0.02 Pa, respectively. The yield point of the gel is more than 2 orders of magnitude larger (see Section 2.2). Hence, the gel behaves elastically.

3.3. Strain Transfer

The average strain transfer from the outer surface of the cable to the optical fiber was calculated according to Equation 8. As the steel wires are embedded in the outer sheath and are not in direct contact with the next inner layer, they are neglected for the calculation of the strain transfer. In case of a cable design as listed in Table 1 and a cable length of 10 m, about 45 % of the strain applied to the outer surface of the cable is transmitted to the optical fiber. For a 100 m long cable, an average of about 95 % of the strain is transmitted to the optical fiber (Figure 3 (a)). For passive seismic recordings, frequencies of less than 10 Hz are of major interest. Assuming a propagation velocity of 3000 m/s, the wavelength is larger than 300 m. For a longitudinal wave half of this length is in compression, half is in extension. Hence, for a cable section of 150 m, on average, about 96 % of the strain applied to the surface of the cable are transmitted to the optical fiber. Figure 3 (b) shows the strain transfer for different wavelength. The -3 dB cut-of wavelength for the transfer function is at a wavelength of about $\approx$22 m.

4. Discussion

Within this study, we used rather conservative estimates on the mechanical properties of individual components to analyse the lower boundary of the strain transfer. For the

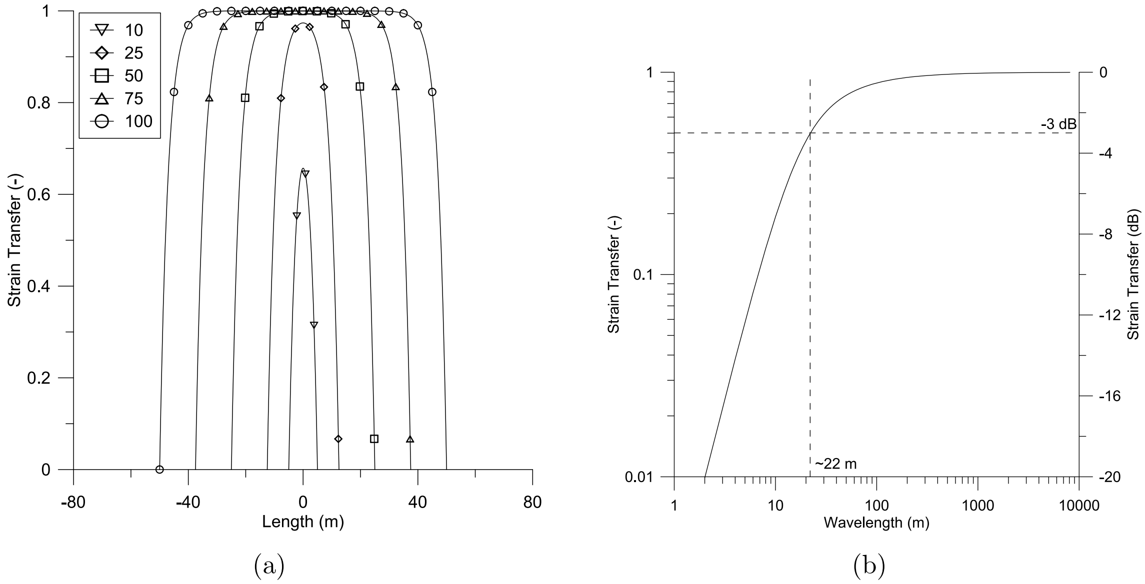

Figure 3. Strain transfer to the optical fiber for the cable design as described in the text. a) Distributed strain transfer along the cable for different cable lengths (10, 25, 50, 75 and 100 m). b) Average strain transfer at different wavelength.

evaluation, a perfect mechanical coupling at all interfaces was assumed. The estimated yield strength of the gel is at the lower boundary of what is reported as an industry standard (Evonik Industries, 2015, and references therein). Generally, optical fibers are overstuffed in a fiber optic cable. In this study, the overstuffing was neglected. In principle, an excess fiber length leads to an increased surface area between optical fiber and gel as well as an increase in the number of contact points between optical fiber and tube wall. Both effects would lead to an increased mechanical coupling between cable structure and fiber as the gel is the weakest component in the set-up and a elastic behaviour has to be guaranteed. However, even with the properties as assumed in this study, the yield strength of the gel is much higher than the expected shear stress.

For the study presented here, the thixothropic behaviour of the gel was neglected. The presented strain transfer, therefore, is valid for a continuous seismic excitation with a maximum strain amplitude of 1 μm/m. Taking into account the thixotropic behaviour of the gel, hence an increased viscosity at the onset of an excitation, a higher strain transfer magnitude can be assumed for event-type excitations, i.e. earthquakes.

A detailed documentation of the deployed cable in Iceland was not available. Hence, the design of the cable was compared to commercially available cable types. For the calculation, therefore, a GYXTW type of cable was used. Diameters and properties of the cable were approximated using a standard cable geometry and standard material properties for each layer. The type of deployment, i.e. embedding in sand, was assumed as a detailed documentation was not accessible.

For seismological applications, the wavelengths of interest are generally rather long. Using the experimental set-up as described in Section 2.4, the transfer function has a

-3 dB cut-of wavelength of about 22 m.

5. Summary and Conclusions

The mechanical coupling between an optical fiber, incorporated in a buried fiber optic cable, and the subsurface was analysed. A simple analytical model was used to calculate the forces needed to stretch the cable. For typical magnitudes of low frequency ground motions, an almost perfect mechanical coupling can be assumed. The presented approach can be used to estimate the transfer function of different fiber optic cable types for seismic applications and beyond.

Acknowledgments

This project has received funding from the European Union's Seventh Framework Programme for research, technological development and demonstration under grant agreement no 608553 (Project IMAGE). The authors would like to thank three anonymous reviewers for their valuable contribution to improve the manuscript.

References

Aki, K. and P. G. Richards (2002). *Quantitative Seismology* (2 ed.). University Science Books.

Ansari, F. and Y. Libo (1998). Mechanics of bond and interface shear transfer in optical fiber sensors. *Journal of Engineering Mechanics 124*(4), 385–394.

Bingham, E. C. (1916). An investigation of the laws of plastic flow. *Bulletin of the Bureau of Standards 13*, 309–353.

Daley, T. M., B. M. Freifeld, J. Ajo-Franklin, S. Dou, R. Pevzner, V. Shulakova, S. Kashikar, D. E. Miller, J. Goetz, J. Henninges, and S. Lueth (2013). Field testing of fiber-optic distributed acoustic sensing (DAS) for subsurface seismic monitoring. *The Leading Edge 32*(6), 699–706.

Evonik Industries (2015). AEROSIL fumed silica for cable gels. Technical Information 1163, Evonik Industries.

Grabe, J. (2012). *Empfehlungen des Arbeitsausschusses "Ufereinfassungen" Häfen und Wasserstraßen EAU 2012*. Ernst W. + Sohn Verlag.

Götz, J., S. Lueth, J. Henninges, and T. Reinsch (2017). Vsp imaging using fibre optic cable as receiver array in four wells simultaneously at the ketzin co2 storage pilot site. In *Proceedings, EAGE/DGG Workshop 2017, Potsdam, Germany*. EAGE Publications BV.

Hartog, A. H., O. Kotov, and L. Liokumovich (2013). The optics of distributed vibration sensing. In *Second EAGE Workshop on Permanent Reservoir Monitoring 2013 – Current and Future Trends*. EAGE.

Herschel, W. H. and R. Bulkley (1926). Konsistenzmessungen von Gummi-Benzollösungen. *Kolloid-Zeitschrift 39*(4), 291–300.

Hooke, R. (1678). *Lectures de Potentia Restitutiva, Or of Spring Explaining the Power of Springing Bodies*. St. Pauls Curch-Yard, London: John Martyn.

Huber, M. (2014). An experimental investigation of thermal effects on the axial resistance to relative ground movement of buried district heating pipes. Master's thesis, University of British Columbia.

Jousset, P., T. Reinsch, J. Henninges, H. Blanck, and T. Ryberg (2016). Strain and ground-motion monitoring at magmatic areas: ultra-long and ultra-dense networks using fibre optic sensing systems. *18*(EGU2016-15707).

Kern GmbH (2016a). Datenblatt Polybutylenterephthalat (PBT).

Kern GmbH (2016b). Datenblatt Polyethylen hoher Dichte (PE-HD).

Khan, S. A., M. A. Maruca, and I. M. Plitz (1991). Rheology of fumed silica dispersions for fiber-optic cables. *Polymer Engineering & Science 31*(24), 1701–1707.

Kuchling, H. (2011). *Taschenbuch der Physik: mit zahlreichen Tabellen*. Fachbuchverl. Leipzig im Carl-Hanser-Verlag.

Li, D., H. Li, L. Ren, and G. Song (2006). Strain transferring analysis of fiber bragg grating sensors. *Optical Engineering 45*(2), 024402–024402–8.

Li, W., C. Cheng, and Y. Lo (2009). Investigation of strain transmission of surface-bonded fbgs used as strain sensors. *Sensors and Actuators A: Physical 149*(2), 201 – 207.

Masoudi, A. and T. P. Newson (2016). Contributed review: Distributed optical fibre dynamic strain sensing. *Review of Scientific Instruments 87*(011501), 9.

Mestayer, J., B. Cox, P. Wills, D. Kiyashchenko, J. Lopez, M. Costello, S. Bourne, G. Ugueto, R. Lupton, G. Solano, D. Hill, and A. Lewis (2011). Field trials of distributed acoustic sensing for geophysical monitoring. *SEG Technical Program Expanded Abstracts 30*(1), 4253–4257.

Mohr, O. (1900). Welche Umstände bedingen die Elastizitätsgrenze und den Bruch eines Materials? *Zeitschrift des Vereins Deutscher Ingenieure 44*, 1524–1530.

Pak, Y. E. (1992). Longitudinal shear transfer in fiber optic sensors. *Smart Materials and Structures 1*(1), 57.

Raab, T., T. Reinsch, P. Jousset, and C. Krawczyk (2017). Multi-station analysis of surface wave dispersion using distributed acoustic fiber optic sensing. In *Proceedings, EAGE/DGG Workshop 2017, Potsdam, Germany*. EAGE Publications BV.

Refi, J. J. (1998). *Fiber Optic Cable*. Geneva, USA: abc Tele Training, Inc.

Reinsch, T., P. Jousset, J. Henninges, and H. Blanck (2016). Distributed acoustic sensing technology in magmatic geothermal areas - first results from a survey in iceland. In *Proceedings, European Geothermal Congress 2017, Strasbourg*.

Schmidt-Hattenberger, C., M. Naumann, and G. Borm (2003). Fiber bragg grating strain measurements in comparison with additional techniques for rock mechanical testing. *IEEE Sensors Journal 3*(1), 50–55.

van Wees, J.-D., J. Hopman, C. Dezayes, R. Vernier, A. Manzella, D. Bruhn, M. Scheck-Wenderoth, O. Flovenz, G. P. Hersir, S. Halldosdottir, and D. Liotta (2015, 4). Image: the eu funded research project integrated methods for advanced geothermal exploration. In *Proceedings World Geothermal Congress 2015*, Melbourne, Australia.